

Abaqus-Based Optimization Study of Cutting TC4 Tool Parameters for Micro-Weaving Tools

Yifan Yuan¹, Hao Xu², Yiqing Huang¹, Shitong Li¹, Yuan Wang^{1,*}

¹College of Machinery and Transportation, Southwest Forestry University, Kunming, Yunnan, China, 650224

²Department of School of Mechanical and Automotive Engineering, Xiamen University of Technology, Xiamen, China, 361024

*Corresponding author: wyuan88@126.com

Abstract: To reduce the machining difficulty of TC4, reduce the main cutting force in the cutting process, reduce the temperature in the cutting area and extend the cutting tool life. Three micro-weaving configurations of rectangular flutes, semi-circular flutes, and triangular flutes were designed on the rake face of the tool, and the rake angle, relief angle, and cutting edge radius of the semi-circular flutes were set at three levels, and the finite element method was used to find the micro-weaving configuration of the tool with the minimum main cutting force and the optimal combination of tool geometry parameters. The results show that under the same cutting conditions, the semicircular fluted micro-weaving tool has the lowest main cutting force among the three micro-weaving profiles; the semicircular fluted micro-weaving tool has 0 °rake angles, 15 °relief angles, and 0.03 mm cutting edge radius, which has the lowest main cutting force.

Keywords: micro-weaving tool; main cutting force; TC4; finite element

1. Introduction

TC4 is a hard-to-machine material that generates high chipping forces in mechanical cutting, which in turn reduces the effectiveness of cutting and shortens the tool life. It has been shown that a reasonable microfabricated cutting tool has excellent characteristics such as high durability and reduced wear [1]. Therefore, the selection of appropriate microfabricated tools for mechanical cutting can significantly improve the frictional state of the cutting zone, reduce tool wear, and significantly improve the surface finish of the workpiece [2].

A lot of research has been carried out by relevant researchers on the cutting performance of micro woven tools. For example, Liu Jia et al [3] carried out a study on the effect of tool micro-pit weaving on tool-chip contact stress distribution and cutting force, and found that micro-pits can reduce front tool surface adhesion, reduce tool-chip contact stress, and further improve tool friction reduction performance. LeQi et al [4] studied the effects of weaving angle, groove spacing, and groove width of turning tool face weaving grooves on the cutting force and cutting temperature during the cutting process of nickel-based alloy and found that the tool face weaving can effectively reduce the cutting force and cutting temperature of the tool. Patel [5] et al. set up micro-weaving grooves with different groove depths, widths, and spacing for turning steel for orthogonal tests and found that the micro-weaving groove parameters have a significant effect on Cutting force, friction along the tool-chip touch and tool loss were all influenced to some extent.

At present, although a lot of results have been achieved in the study of micro-weaving tools, most of them focus on the cutting of steel, while the machining of TC4 is still limited [6]. Therefore, in this paper, we propose to design three tools with different micro-weave profiles, compare the cutting force magnitude by the limit element analysis under the same cutting parameters to obtain the optimal micro-weaving profile, and then use the orthogonal experimental method to find the optimal geometric parameters of the tool with the optimal micro-weaving profile, aiming to provide some theoretical reference for the design of the micro-weaving profile of the tool.

2. Finite element simulation model and micro-weaving tool design

2.1 Geometric modeling

Usually, when the cutting width is more than 5 times the cutting thickness, the overall cutting process shows more obvious plane strain characteristics, and then the whole process of cutting can be treated as a plane strain problem, and the three-dimensional cutting process is approximated by the two-dimensional cutting process [7]. To simplify the model and reduce the calculation time, this paper adopts a two-dimensional cutting model to approximate the replacement of the three-dimensional cutting process and establishes a two-dimensional cutting model to simulate the cutting process of TC4. In the cutting process, the length and width of the workpiece are 1.5 mm and 0.8 mm, respectively. the tool material is selected as YG8, the rake angle of the tool is 5°, the relief angle is 7°, the radius of the cutting edge is 0.03 mm, and the micro-weaving morphology is designed on the rake face, as shown in Figure 1(a), and the cutting process model is established as in Figure 1(b). In Figure 1(a), s-weaving groove spacing, w-weaving groove width, d-weaving groove depth.

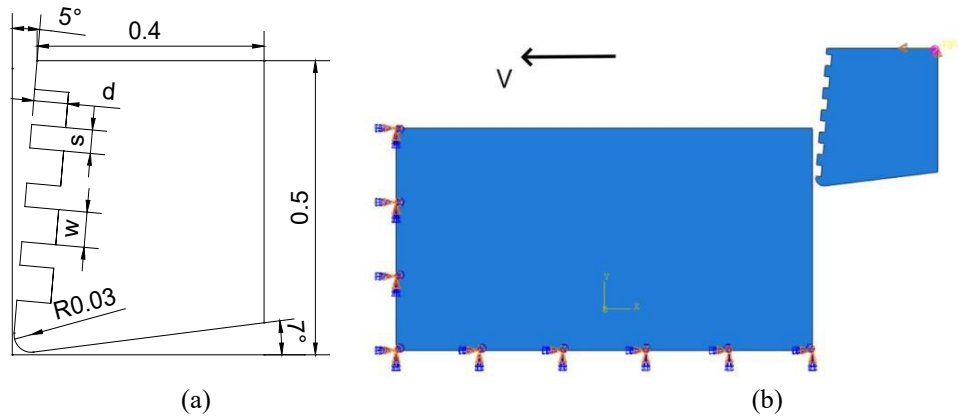


Figure 1: Micro-weaving tool (a) and cutting model (b)

2.2 Johnson-Cook model

When metal materials are cut and machined, they usually have elasticity and mobility under high deformation and high strain rate, and it is crucial to fully consider the constraints of various factors on the flow stress of the workpiece to establish a proper material flow stress model in the finite element simulation experiment [8]. The materials are different and their applicable material models are different, and in this paper, the Johnson-Cook material intentional model, which is very commonly used at this stage, is selected, and its model equation is:

$$\sigma = (A + B \cdot \epsilon^n) \left(1 + C \cdot \ln \left(\frac{\dot{\epsilon}}{\dot{\epsilon}_0} \right) \right) \left(1 - \left(\frac{T - T_r}{T_m - T_r} \right)^m \right) \quad (1)$$

Where A, B, C, m, and n are constants, related to the selected material type, and the TC4 model parameters of reference [8] are listed in Table 1.

Table 1: Parameters of the Johnson-Cook material ontology model for TC4[8]

A(MPa)	B(MPa)	n	C	m
862	331	0.2	0.035	0.8

2.3 Chip separation guidelines

The Johnson-Cook shear fracture model was chosen to simulate the separation process of chips and workpieces during the cutting process, and the mathematical expression of the failure parameter is.

$$\omega = \sum \frac{\Delta \epsilon^{pl}}{\epsilon_f^{pl}} \quad (2)$$

Where, $\Delta \epsilon^{pl}$ -plastic strain increment; ϵ_f^{pl} -failure strain, which can be expressed as

$$\varepsilon_f^{pl} = \left[d_1 + d_2 \exp d_3 \left(\frac{\sigma_m}{\bar{\sigma}} \right) \right] \left(1 + d_4 \ln \frac{\varepsilon^{pl}}{\dot{\varepsilon}_0} \right) \left[1 - d_5 \left(\frac{T - T_0}{T_{melt} - T_0} \right) \right] \quad (3)$$

Where, the σ_m -average value of principal stress; ε^{pl} -strain rate; T_{melt} -material melting temperature, the value of which is taken as 1560°C; $d_1 - d_5$ is the material failure parameter, listed in Table 2.

Table 2: Specific values of TC4 material parameters

d_1	d_2	d_3	d_4	d_5
-0.09	0.25	-0.5	0.014	3.87

2.4 Micro-weaving tool design

Figure 2 shows the designed micro-weaving tool with rectangular flutes, semi-circular flutes, and right-angle triangular flutes, and the shape after finite element meshing (meshing settings: choose Quad for element shape type and Free for mesh Technique), the geometric parameters of the micro-weaving tool and the cutting amount for the finite element simulation are shown in Table 3, and the friction factor is taken to be 0.3. The geometrical parameters of the micro-weaving tool and the cutting amount for the finite element simulation are shown in Table 3, and the friction factor is 0.3.

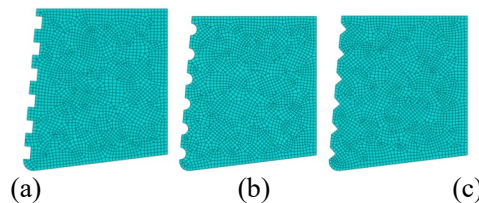


Figure 2: Micro-weaving tools with different morphologies: a-rectangular notch, b-semi-circular notch, and c-right-angle triangle

Table 3: Micro-fabrication tool parameters and cutting dosage

Spacing s	Width w	Depth d	Rake angle	Relief angle	Feed amount	Cutting speed	Cutting depth
0.04 mm	0.04 mm	0.02 mm	5°	7°	1.5 mm/s	1.5 mm/s	0.2 mm

3. Finite element simulation results and analysis

3.1 Analysis of cutting forces

Cutting force is an important variable in mechanical cutting machining, and its magnitude directly affects the temperature level in the cutting zone, which in turn determines the tool life and workpiece surface machining quality to a certain extent. From the finite element simulation, it is known that the cutting phase in 0.4-0.8s is the stable machining phase, and the main cutting force of this duration is taken within Table 4. According to the table, the average main cutting force of the semicircular fluted tool is 223.04 N, which is 0.18% and 1.86% less than the 223.88 N of the rectangular fluted tool and 227.19 N of the triangular fluted tool, respectively, which shows that the semicircular fluted micro-weaving tool can reduce the main cutting force. This is because the chips formed on the front face of the semi-circular fluted micro-weaving tool are easier to be discharged during the cutting process, and are not easily retained in the groove of the front face, forming chip retention and increasing the friction between the tool and chips.

Table 4: Average value of main cutting force at the stabilization stage of different weave morphology

Microfabricated morphology	The average value of main cutting force(N)
Rectangular recess	223.88
Triangular recess	227.19
Semicircular recess	223.04

3.2 Orthogonal experiments on the effect of tool geometry parameters on main cutting forces

From the finite element simulation of three Microfabricated morphology on the main cutting force, it is known that the semi-circular fluted weave tool has the smallest main cutting force, and thus the semi-circular fluted micro-weaving tool is selected to study the effect of tool geometric parameters on the main cutting force. L9(34) was chosen to establish orthogonal tables for simulation experiments with three variables of tool rake angle, tool back angle, and cutting edge radius as independent variables, respectively. The variable values of tool rake angle were taken as 0°, 5°, and 10°, back angle was taken as 5°, 10° and 15°, and the cutting edge radius were taken as 0.01 mm, 0.03 mm and 0.05 mm, respectively. cutting amount was fixed, cutting speed 1.5 mm/s, feed 1.5 mm/s, and cutting depth 0.2 mm.

3.2.1 Design of cutting orthogonal experiments

The finite element simulation to explore the effect of tool geometric parameters on the main cutting force involves three factors, namely, tool rake angle, back angle, and cutting edge radius, with three variables set for each factor, and the orthogonal table for the finite element simulation is shown in Table 5.

Table 5: Orthogonal experiment set up the orthogonal table

Level	Rake angle of the tool (°)	Relief angle of the tool (°)	The radius of cutting edge(mm)
Level 1	0	5	0.01
Level 2	5	10	0.03
Level 3	10	15	0.05

3.2.2 Simulation results and analysis

A set of main cutting forces can be derived for each set of experiments. Selected data from the stabilization process were used to derive the average values of the main cutting forces and are listed in Table 6.

Table 6: Cutting force test results and analysis of orthogonal test

Experiment serial number	Factors			The average value of main cutting force(N)
	Level of the rake angle of the tool (A)	Level of the relief angle of the tool(B)	Level of cutting- edge radius (C)	
1	1	1	1	234.36
2	1	2	2	227.48
3	1	3	3	244.07
4	2	1	2	225.90
5	2	2	3	252.87
6	2	3	1	232.20
7	3	1	3	260.08
8	3	2	1	247.11
9	3	3	2	239.88
K1	705.91	720.34	713.67	
K2	710.97	727.46	693.26	
K3	747.07	716.15	757.02	
K1	235.30	240.11	237.89	
K2	236.99	242.49	231.09	
K3	249.02	238.72	252.34	
Range	13.72	3.77	21.25	
Order of priority		C>A>B		
Superior level	A ₁	B ₃	C ₂	
Superior Combination		A ₁ B ₃ C ₂		

The test results in Table 6 were subjected to extreme difference analysis, and comparing the size of R values, it can be seen that C>A>B. Therefore, the main order of the influence of the test factors on the test index is C→A→B, that is, the cutting edge radius has the greatest influence, followed by the tool rake angle, while the tool back angle has the least influence. And it can be seen from Table 6 that the optimal

combination in the test is A1B3C2, when the tool rake angle is 0° , the back angle is 15° , the cutting edge radius is 0.03 mm, and the micro-weaving configuration profile is the semi-circular groove, the average main cutting force is the smallest.

4. Conclusions

1) Among the three types of micro-weaving tools with rectangular recess, triangular recess, and semicircular recess, the semicircular recess micro-weaving tool has the smallest main cutting force, i.e., the best performance when cutting TC4 using the semicircular micro-weaving tool.

2) In the semi-circular fluted micro-weaving tool with 0° rake angle and 15° relief angle and 0.03 mm cutting edge radius, the main cutting force is the smallest.

References

- [1] Deng Jieyong, Zheng Qingchun, Hu Yahui, et al. Study on cutting mechanism of micro-weaving tools based on ABAQUS. *Tool Technology*, 2016, 50(11):23-27.
- [2] Qi Baoyun, Li Liang, He Ning, et al. Experimental study of orthogonal cutting of Ti6Al4V with micro-weaving tools. *Journal of Tribology*, 2011, 31(04):346-351.
- [3] Liu Jia, Yu Huadong, Yu Zhanjiang et al. Analysis of orthogonal micro-cutting performance of titanium alloy under micro weaving-derived cutting. *Tool Technology*, 2021, 55(09):47-53.
- [4] Le Qizhong, Lei Xuelin, Wu Botao, et al. Optimization of surface groove weaving parameters of high-temperature alloy cutting tools. *Machine Tools and Hydraulics*, 2021, 49(12):6-11.
- [5] Kaushalendra V. Patel, Suril R. Shah, Tuğrul Özel. orthogonal cutting of alloy steel 4340 with micro-grooved cutting tools. *Procedia CIRP*, 2019, 82.
- [6] Liu W, Liu SH, Liang GQ, et al. Simulation analysis of cutting performance and friction reduction effect of micro-woven cutting tools. *Surface Technology*, 2022, 51(02):338-346.
- [7] Zhao Tengjun. *Application of ABAQUS in mechanical engineering*. Beijing: China Water Conservancy and Hydropower Press, 2007:67-68.
- [8] Yugang Ye, Yan Yin. The establishment of a dynamic constitutive model for cutting of titanium alloy TC4 by finite element simulation. *Ordnance Material Science and Engineering*, 2009:32(6):35-38.